

Time-invariant person-specific frequency templates in human brain activity

Itai Doron¹, Eyal Hulata¹, Itay Baruchi¹, Vernon L. Towle², and Eshel Ben-Jacob¹

¹*School of Physics and Astronomy, Raymond & Beverly Sackler Faculty of Exact Sciences, Tel-Aviv University, Tel-Aviv 69978, Israel* and*

²*Department of Neurology, BH2030, The University of Chicago, 5841 South Maryland Avenue, Chicago, Illinois 60637, USA*

The various human brain tasks are performed at different locations and time scales. Yet, we discovered the existence of time-invariant (above an essential time scale) partitioning of the brain activity into person-specific frequency bands. For that, we perform temporal and ensemble averaging of best wavelet packet bases from multi-electrode EEG recordings. These personal frequency-bands provide new templates for quantitative analyses of brain function, e.g., normal vs. epileptic activity.

Keywords: wavelet packets, best basis, electrocorticogram

Introduction. The various brain tasks (cognitive, sensory, motor etc.) are performed simultaneously in many locations and operate at different time scales. In order to quantify abnormal vs. normal brain function, as in the case of epilepsy, it is necessary to develop time-invariant templates for characterization of normal behavior. The challenge is to decipher time-invariant features from multi-electrode EEG recordings of brain activity. Moreover, from Physics perspective, it is not clear a priori that time-invariant elements do exist since the activity is inherently nonergodic.

Here we present a new approach of temporal and ensemble averaging of best-bases constructed from Wavelet Packets Decomposition (WPD) of the recorded brain activity. The approach is illustrated via the analysis of subdural EEG (ECoG) recordings from grids of electrodes that are placed directly on the surface of the cortex (Fig. 1). Such recordings are performed to analyze the brain activity of epileptic patients under chronic evaluation before resection surgery to remove the epileptic focus or foci [1, 2, 3, 4]. Using this approach, we discovered the existence of time-invariant person-specific frequency bands above an essential time scale of about 2.5 minutes. We devised a quantitative measure for comparison between WPD bases. Our new analysis approach can help, for example, in the identification of the epileptic foci and in the development of quantitative analysis methods for early warning of epileptic seizures. As a self-consistency test that the frequency bands are not an artifact of the analysis, we show that the same templates are obtained for subdural and scalp EEG recordings of the same person.

The recorded ECoG signals. The signals analyzed here are ECoG recordings from grids of typically ~ 100 electrodes. These recordings are obtained from epileptic patients undergoing chronic evaluation for surgery. The electrodes are spatially distributed over the suspected focal region, so that the focus or foci could be localized by analyzing the ensemble of signals. The amplitude of the signals records the electrical voltage at each electrode (arguably recording local field potentials [LFP] [5]).

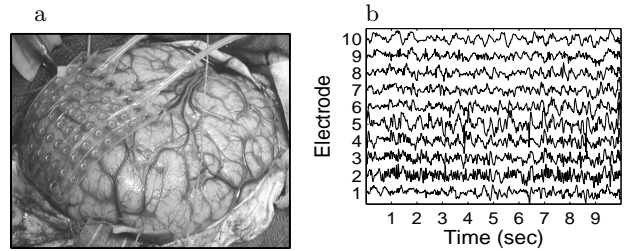


FIG. 1: : (a) **Subdural EEG (ECoG) grid of electrodes** placed on the pial surface of the brain for chronic evaluation of epileptic patients before surgical resection. (b) **Voltage traces of ECoG signals.** A 10 second time window display of voltage traces of 10 electrodes, taken from a multi-electrode recording of 96 electrodes.

The voltage signals are simultaneously digitized at 112Hz (sampling time interval $\Delta t_{min} \simeq 9$ mSec) with a lowpass filter up to 40Hz. The analysis is usually performed in time windows of $N_{bin} = 1024$ samples.

Time-Frequency analysis. In general, the possible time intervals for a recorded sequence of N_{bin} elements can range from $\Delta t_{min} = 1$ (in units of the sampling time interval) to $\Delta t_{max} = N_{bin}$. In principle, one can extract information about N_{bin} time intervals at each of the N_{bin} temporal locations along the sequence. However, such an N_{bin}^2 matrix for a sequence of only N_{bin} data samples must contain redundant information (i.e. over-complete representation of the recorded sequence). In order to avoid such redundancy, only N_{bin} time-frequency locations should be selected, subject to the uncertainty constraint between time and frequency resolutions - $\Delta t \cdot \Delta f = 1$.

Since there are N_{bin} corresponding frequency bands, ranging from $\Delta f_{min} = 1/N_{bin}$ to $\Delta f_{max} = 1$ (in units of the Nyquist frequency), each location can be assigned a local relative resolution $\Delta t/\Delta f$ out of $N_R = 1 + \log_2(N_{bin})$ possible ratios (for simplicity, N_{bin} of the sequences considered here are in factors of 2). It is convenient to illustrate both constraints as tiling of the time-frequency plane with N_{bin} rectangles, each with its own aspect ratio (height Δf and width Δt), representing the

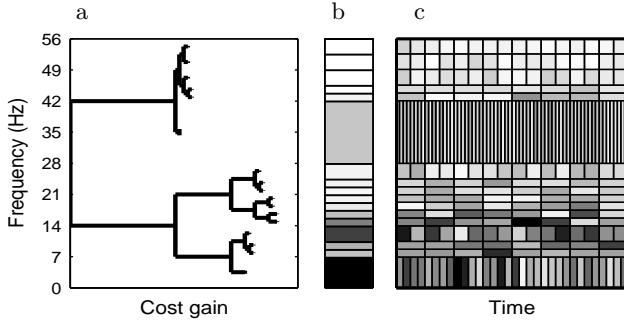


FIG. 2: An illustration of the Wavelet Packets Decomposition (WPD) for a typical signal recorded from a single electrode. (a) A binary tree representation of the best basis obtained by WPD. Each node in the tree represents a basis frequency band. The vertical axis represents the frequency while the horizontal axis represents the information cost gain of the basis frequency band blocks. (b) The corresponding information distribution in the frequency bands of the best basis (darker shades represent more information). (c) 2-D tiling representation of the WPD of the signal (darker shades represent larger wavelet packet coefficients). The vertical axis represents the frequency while the horizontal axis represents the time. If the rectangles were colored according to their information cost contribution then the information distribution shown in (b) would simply be a sum over the rows of the basis coefficients.

relative resolutions in time and frequency [6, 7].

The WPD as a binary tree. The Wavelet Packets Decomposition we use here was devised to partition (tile) the time-frequency plane into such rectangles (referred to as 'information cells' or 'Heisenberg boxes') [8, 9, 10]. Each possible combination of N_{bin} non-overlapping tiles that geometrically covers the entire corresponding time-frequency plane can serve as a complete basis spanning the recorded sequence.

The WPD is computed by iterating a set of lowpass and highpass filters (H and G respectively). The functions underlying the expansions of H and G are "wavelets" ("mother") and "scaling" ("father") functions [11]. At each iteration, the wavelet packet coefficients are computed by convoluting the signal with the filters. Here we utilize the WPD using the 'Coiflet' of order 1 as a "mother" wavelet (smallest time support of all 'Coiflets') [12, 13, 14, 15].

Using the Best Basis algorithm. The WPD generates an over-complete representation of the signal. The challenge is to select, out of all possible representations, the one that is the most efficient in extracting the features of interest. The Best Basis algorithm is a method for selecting a basis that spans the signal with a small number of significant packets [8, 10]. For that, each wavelet packet function is assigned an information cost value $M_q(q) = -q \cdot \log_2(q)$ where q is the normalized energy of the wavelet packet. The total information cost of a frequency subband is obtained by summing over all the

packets in the subband:

$$M_{subband} = \sum_{k=1}^K M_q(q_k). \quad (1)$$

Viewing the frequency subbands as nodes in a binary tree, the selection of the best basis is similar to a binary tree search. Starting from the lowest level bands, we select for each pair of subbands either the two subbands or their joint "parent" band, whichever has the lower information cost. The process is repeated at subsequent levels, going up the scales, back to the global root. Doing so, we select the set of subbands with the lowest possible information cost (Fig. 2).

Bases Similarity Measure. Every wavelet packets basis can be described by the frequency subbands partitioning and the corresponding information cost of every one of the subbands. We suggest using the following similarity measure, annotated SM , for comparison between decomposition bases - $basis1$ and $basis2$:

$$SM = \frac{\sum_{n1=n2} (M_{n1} + M_{n2})}{\sum_{n1} M_{n1} + \sum_{n2} M_{n2}}, \quad (2)$$

where M_{n1} and M_{n2} are the information cost of subbands $n1$ and $n2$ for $basis1$ and $basis2$, respectively. The summation in the nominator is over all the common subbands of the two bases. The idea is to compare the information cost included in the similar subbands to the total information cost. Note, that the measure assumes values between 0 (if the bases are totally dissimilar) and 1 (if they are exactly the same).

The Ensemble Best Basis of multi-electrodes recordings. In Figs. 3a and 3b we show an example of the evaluated Best Bases for the recordings from two different electrodes at consecutive time windows (~ 10 seconds). As can be seen in these figures, the Best Bases differ from electrode to electrode ($SM = 0.46 \pm 0.20$ between these electrodes) and also vary between consecutive time windows for the same electrode ($SM = 0.58 \pm 0.12$ [Fig. 3a] and $SM = 0.63 \pm 0.25$ [Fig. 3b]). Looking for invariant Best Bases, we proceed to evaluate an ensemble Best Basis for all the electrodes. Following previously devised methods [16, 17, 18, 19], we average over the information cost binary tree of each of the L recorded signals in the ensemble. This is done by first calculating the information cost of all the nodes in the binary WPD tree for each of the signals. Next, we evaluate the mean information cost of every node for the L signals by simple averaging. Then we apply the Best Basis algorithm to the mean values tree. Thus, we obtain a basis that may not be optimal for each signal, but rather underlines the mean content of the ensemble. The nonergodic nature of the brain activity is reflected in the fact that the resulting ensemble best basis (EBB) varies between successive short time windows ($SM = 0.65 \pm 0.33$). Similarly, if we start with temporal coarse-graining of the Best Bases for

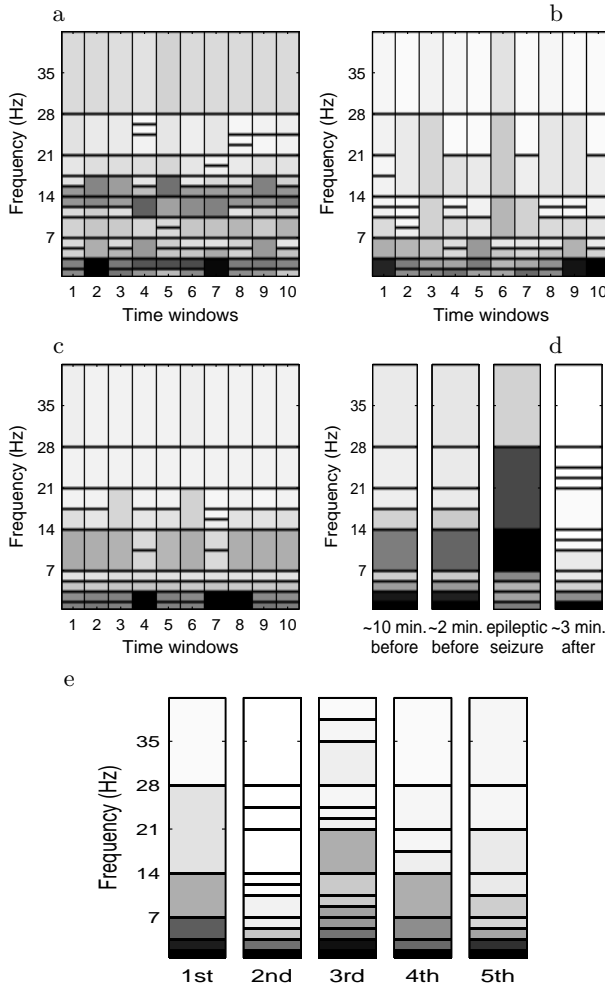


FIG. 3: Person-specific frequency bands. The frequency subbands division of the best basis of a single ECoG electrode signal can change over time, as can be seen in (a) and (b), when calculated at 10 consecutive time windows of 9 seconds each (we used only 5 levels of decomposition, to avoid a large influence due to a negligent number of coefficients, when using short time windows). Comparing (a) to (b), it is evident that the frequency subbands division is also distinct for the different spatial locations. Even the ensemble best basis of all the 96 ensemble electrodes, as shown in (c), does not yield time-invariant partitioning into frequency subbands. However, temporal coarse-graining of the ensemble best basis by averaging over time windows of approximately 2.5 minutes produces robust frequency bands that are time-invariant for long periods (over 10 minutes). This robustness is presented in (d) by examples from the same recordings of such time-invariant partitioning into frequency bands (before the seizure) [21]. Nonetheless, the large diversity between individuals, which can be observed in the 5 examples in (e), leads us to regard them as person-specific frequency bands partitioning or spectral signatures.

the individual electrodes, the resulting Best Bases are different from each other and from the Ensemble Best Bases. This is a reflection of the inherent nonergodicity of the brain activity.

Time-Invariant Best Bases. However, we did discover the existence of an underlying time-invariant ($SM \simeq 1$) Best Basis in the nonergodic activity. This basis is dis-

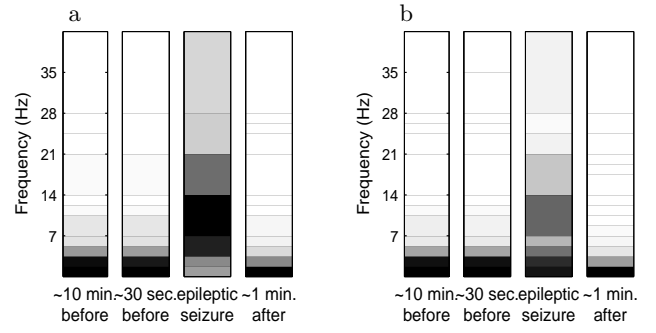


FIG. 4: The frequency templates - before, during and after epileptic seizure. (a) The stability of the frequency template of the ECoG recording is demonstrated for time intervals of approximately 2.5 minutes each, 10 minutes before the seizure onset and 30 seconds before the seizure onset. During the seizure, the energy distribution of the signals changes dramatically [23]. After the seizure, the energy distribution changes again, as the energy in the high frequencies decreases. (b) Preliminary analysis of scalp EEG signals from the same recording of (a) shows the same frequency template (inter-ictal and post-ictal) and the same temporal changes in the energy distribution.

covered by combining ensemble averaging and temporal coarse-graining over a new essential time scale. Namely, by temporal coarse-graining of the short time EBBs over a time window wider than an essential time scale (about 2.5 minutes) [20]. The latter satisfies the requirement that the SM between EBBs at different time segments is larger than 0.95.

As shown in Fig. 3d, the resulting Best Basis is time-invariant for recorded periods that are much longer than the essential time scale [21]. Hence, the time-invariant bases can be used as a frequency decomposition template for analyzing the recorded brain activity at different times and locations [22].

Person-Specific Frequency Bands. Applying the new spatio-temporal averaging of the Best Bases to the recordings from different persons (we analyzed recordings from 12 persons), we found that each has its own specific time-invariant Best Basis with its own characteristic features, as illustrated in Fig. 3e. We emphasize that each of the personal bases bears resemblance to the classical EEG frequency bands, yet has its own specific significant deviations from it. Reflecting this notion, we note that the inter-patient similarity is $SM = 0.75 \pm 0.16$ for these examples, which is higher than the similarity between the variations of an EBB of a single patient over short time windows. However, this inter-patient similarity is significantly lower than $SM \simeq 1$, which is measured for bases of different time windows of recordings of a single patient above an essential time scale, and could not be considered as invariant. We propose that the frequency bands are personal specific spectral signatures that can be used in patient-specific diagnosis of recorded brain activity.

Self-Consistency Test. To further substantiate this idea (and that the calculated frequency bands are not an

artifact), we show a comparison of the frequency bands calculated in parallel, for the same person, both from ECoG and scalp EEG recordings. As illustrated in Fig. 4, between seizure episodes (inter-ictal) the calculated frequency bands are almost identical ($SM \simeq 1$). We also show that the frequency partitioning changes during the seizure (ictal) episodes. Hence, we expect that a decomposition of the ictal activity according to the inter-ictal bands can help in seizure diagnosis.

Conclusions. These results illustrate the potential value of the personal best-basis to serve as a template for quantitative analysis of the epileptic activity [24]. For example, the ictal activity can be decomposed according to the inter-ictal bands during the chronic monitoring of the brain activity. Our new analysis approach can help, for example, in the identification of the epileptic foci. It can also be used to develop quantitative person-specific analysis for early warning of epileptic seizures [25, 26]. Beyond recorded brain activity, we expect the new approach to be helpful in revealing the existence of essential time scales and time-invariant frequency decomposition templates in a wide class of other nonergodic biological systems with multi-time scale dynamics. As in the case of the brain, we expect that revealing such hidden templates can help in analyzing variations in the systems function and performance.

* Electronic address: eshel@tamar.tau.ac.il

- [1] The occurrence of epilepsy is estimated to affect about 1% of the world population [2]. With the aid of anti-epileptic drugs, approximately 70% of all epileptic patients can be kept seizure-free. But for the remaining 30%, the best possible treatment is surgical resection of the focus [3]. A challenging task facing epileptologists is the precise identification of the focus regions that should be removed [4]. When the localization of the region remains uncertain after conventional, noninvasive measurements such as EEG and MEG, better localization is obtained using invasive electrocorticogram (ECoG).
- [2] B. Litt and J. Echauz, THE LANCET Neurology, 1 (1): 22-30 (2002).
- [3] S. J. Schiff, Nature Medicine 4 (10): 1117-1118 (1998).
- [4] V. L. Towle et al., *Epilepsy as a Dynamic Disease*, (P. Jung, J. Milton eds.), Springer: Berlin (2002).
- [5] J. Ph. Lachaux, D. Rudrauf, and P. Kahane, J. Physiology, 97: 613-628 (2003).
- [6] E. Hulata, I. Baruchi, R. Segev, Y. Shapira, and E. Ben-Jacob, Phys. Rev. Lett., 92(19), 198105 (2004).
- [7] E. Hulata, V. Volman, and E. Ben-Jacob, J. Natural Computing, 4, 363-386 (2005) .
- [8] R. R. Coifman and M. V. Wickerhauser, IEEE Trans. Inf. Theory., 38(2), 713-718 (1992).
- [9] S. Mallat, *A wavelet tour of signal processing (2nd Ed.)*, Academic Press (1999).
- [10] R. R. Coifman and M. V. Wickerhauser, Proc. Symp. in Applied Mathematics, 47, 119-153 (1993).
- [11] M. V. Wickerhauser, Proc. Symp. in Applied Mathematics, 47, 155-171 (1993).
- [12] Since the spike is such an important aspect of epileptic activity [13], we used a wavelet packet which allows very high resolution time localization of spikes.
- [13] S. Blanco et al., Phys. Rev. E, 57(1), 932-940 (1998).
- [14] J. Gutiérrez, R. Alcántara, and V. Medina, Medical Engineering & Physics, 23, 623-631 (2001).
- [15] In the first iteration, the time-frequency plane is divided into two halves: the low frequencies subband and the high frequencies subband. At each iteration the subbands from the previous iteration are divided again into a low frequencies half and a high frequencies half. This procedure is repeated until the highest frequency resolution ($\Delta f_{min} = 1/N_{bin}$) is reached. Each iteration of the filters correspond to a division of a "parent" tree node into two "children" as shown in Fig. 2a.
- [16] S. Mallat, G. Papanicolaou, and Z. Zhang, *The Annals of Statistics*, 26(1), 1-47, Academic Press (1998).
- [17] N. Saito, Wavelet Applications in *Signal and Image Processing VI*, (A.F.Laine, M.A.Unser, A.Aldroubi eds.), Proc. SPIE 3458, 24-37 (1998).
- [18] R. R. Coifman and N. Saito, Proc.IEEE International Symposium on Time-Frequency and Time-Scale Analysis, 129-132, IEEE Signal Processing Society (1996).
- [19] N. Saito and R. R. Coifman, J. Mathematical Imaging and Vision, 5, 337-358 (1995).
- [20] We checked that the way that the averaging is done (number of time windows, their size etc.) is not important, provided that it is done over intervals longer than 2.5 minutes.
- [21] When available, we compared two recordings: the second recorded 3 hours after the first. The similarity between the corresponding Best Bases was approximately 1.
- [22] R. Salvador et al., Cerebral Cortex, 15 (9): 1332-1342 (2005).
- [23] A. D. Krystal, R. Prado, and M. West, Clin Neurophysiol, 110, 2197-2206 (1999).
- [24] B. Percha et al., Phys. Rev. E 72, 031909 (2005).
- [25] K. Lehnertz and C. E. Elger, Phys. Rev. Lett., 80(22), 5019 (1998).
- [26] J. Arnhold et al., Physica D, 134, 419-430 (1999).